Assessment of the ability of poly-L-lysine-poly(ethylene glycol) (PLL-PEG) hydrogels to support the growth of U87-MG and F98 glioma tumor cells: Research Article

Article *in* Journal of Applied Polymer Science · February 2018
DOI: 10.1002/app.46287

7 authors, including:

Emilie Gontran
French Institute of Health and Medical Research
8 PUBLICATIONS **0** CITATIONS
SEE PROFILE

Marjorie Juchaux
CNRS, Orsay, France
36 PUBLICATIONS **151** CITATIONS
SEE PROFILE

Sergei G Kruglik
Pierre and Marie Curie University - Paris 6
123 PUBLICATIONS **1,281** CITATIONS
SEE PROFILE

Olivier Seksek
French National Centre for Scientific Research
44 PUBLICATIONS **1,830** CITATIONS
SEE PROFILE

Journal of Applied Polymer Science

Assessment of the ability of poly-L-lysine-poly(ethylene glycol) (PLL-PEG) hydrogels to support the growth of U87-MG and F98 glioma tumor cells

Emilie Gontran,[1] Marjorie Juchaux,[1] Christophe Deroulers,[1] Sergei Kruglik,[2] Nicolas Huang,[3] Mathilde Badoual,[1] Olivier Seksek[1]

[1]Imagerie et Modélisation en Neurobiologie et Cancérologie (IMNC), CNRS UMR 8165, Univ Paris-Sud, Univ Paris Diderot, Orsay 91405, France

[2]Laboratoire Jean Perrin, Sorbonne Universités, UPMC Univ Paris 06, CNRS UMR 8237, Paris 75005, France

[3]Institut Galien Paris-Sud, CNRS UMR 8612, Univ Paris-Sud, Université Paris-Saclay, Faculté de Pharmacie, 5 rue J.B. Clément, Châtenay-Malabry 92296, France

Correspondence to: O. Seksek (E-mail: seksek@imnc.in2p3.fr)

ABSTRACT: Biomaterials that provide 3D-like *in vitro* cell survival and proliferation are increasingly used to mimic the extracellular microenvironment in the context of a better understanding of tumorigenesis. In this study, a simple, affordable and fast technique to fabricate hydrogel matrices composed of poly(ethylene glycol) (PEG) and poly-L-lysine (PLL) (as cell-adhesive factor) were used to provide *in vitro* glioma cell growth. After UV photopolymerization of a precursor solution containing PEG-diacrylate and easily obtainable PLL-acrylate derivatives, F98 and U87-MG cells (rat and human glioblastoma cell lines, respectively) were grown on top of different substrates that consist of combinations of PEG/PLL hydrogels and spontaneously formed cell aggregates of homogeneous sizes. Depending on the cell type, PEG and PLL concentrations, the cell aggregates patterns were different. The optimal combination to obtain cell survival and proliferation for both cell lines was determined as 3% PEG (w/v) and 0.001% PLL (w/v). This technique was also used to assess the efficacy of temozolomide and should be adaptable to other cancer cell lines to follow pseudo-tumor growth *in vitro*. © 2018 Wiley Periodicals, Inc. J. Appl. Polym. Sci. **2018**, *135*, 46287.

KEYWORDS: biomaterials; biomimetic; gels; microscopy; photopolymerization

Received 27 September 2017; accepted 20 January 2018

DOI: 10.1002/app.46287

INTRODUCTION

Malignant gliomas are highly invasive primary brain tumors and they are classified according to grades, grade IV tumors (or glioblastoma multiforme, GBM) being the most aggressive type, corresponding to a patient survival of 6 months to 2 years.[1] They are characterized by their diffuse infiltration through migration into the normal brain parenchyma and interaction with the extracellular matrix (ECM), leading to new tumor foci.[2] This invasion explains the failure of standard brain tumor therapies. During these migration processes, glioma cells migrate inside the cerebral tissue, which is a very soft biological tissue with stiffness ranging from 100 Pa to 1 kPa.[3] Thus, to study glioma cells *in vitro* with growing conditions as comparable as *in vivo* environment, and possibly the effect of drugs for the development of an efficient therapy, it is of primary importance to create a brain-like milieu with similar mechanical properties than the cerebral tissue.[4,5]

In this research line, an important effort has been made to build biomimetic ECM in gel structures with physicochemical properties similar as those of the brain.[6,7] Two main strategies are under investigation: gels based either on naturally derived macromolecules or on synthetic polymers. In the first approach, the touchstone is the mouse sarcoma cancer cells extract (Matrigel, Corning Life Sciences), a complex mixture providing an ECM naturally enriched in compounds promoting cell adhesion and cell survival such as laminin, collagen, growth factors and enzymes. While this preparation has the inherent advantage of a complete biocompatibility and *in vivo*-like molecular architecture, it has some drawbacks: relatively high cost, lack of fine control of their physicochemical properties, batch-to-batch variability, uncontrolled degradation process and time alteration. Therefore, new strategies have emerged by using specific natural or synthetic polymers, that is, forming hydrogels that are hydrophilic polymer networks with porous structure containing a

high water volume (interesting for nutrients distribution to cells) and with a controlled structure that might match natural matrix properties and synthetized by chemical methods using synthetic polymers.[8]

So far, gliomas have been studied in hydrogels with naturally derived hyaluronan [hyaluronic acid (HA)], which is the predominant brain matrix component. However, the HA-based hydrogel synthesis mode did not allow for full control of matrix properties. Poly(ethylene glycol) (PEG)-methacrylate (MA) and gelatin-MA hydrogels in combination with methacrylated HA showed glioma cell clustering and glioma malignancy markers expression in comparison with non-functionalized scaffolds.[9] However, viability assays showed limited cell proliferation, which is likely due to toxicity arising from the photopolymerization method using a 10 min UV exposure. In another work, PEG-based hydrogels were covalently linked with cell adhesion peptides and MMP residues. HA molecules were physically entrapped within the hydrogels structures to provide glioma cell growth.[10] Nevertheless, this hydrogel did not allow for long-term studies either since biochemical effects would be changed by HA dilution through cell medium rinsing. Ananthanarayanan *et al.*[11] used simple methacrylated HA hydrogels with adsorbed RGD peptides crosslinked with DL-dithiothreitol (DTT) to study the effects of matrix stiffness on human glioblastoma cells. In this case, DTT crosslinking occurs at pH higher than 7, which renders hydrogel properties depending on the cell metabolization with degradation of crosslinker residues upon cell medium acidification. Finally, Oh *et al.*[12] presented a dual UV-ionic PEG/alginate hydrogels for creating tumor spheres from glioma cancer stem cells (CSCs), allowing 3D studies of therapeutic CSCs resistance, self-renewal, and differentiation, but with some issues with the chemical stability of the hydrogel matrix. Therefore, all these hydrogel formulations that aimed at mimicking brain ECM composition, used HA in order to reproduce *in vivo* macroporos structure of brain tissue. But such HA crosslinked hydrogels using ionic polymerization still remains largely unstable upon pH variations through cell metabolization.[13] Hence, it limits long-term cell studies because of the medium acidification that accompanies cells proliferation.

To achieve independently tunable biochemical and mechanical properties, we chose to focus on a PEG-based hydrogel. Indeed, the advantages of PEG-based hydrogels regarding to natural brain matrix properties, and in comparison with HA, are that PEG is a well-characterized molecule due to its easily controllable and stable properties: PEG-based hydrogels exhibit elastic mechanical properties comparable with HA, and adaptable over a wide range of elastic moduli matching that of the extracellular brain matrix[14,15]; PEG characterization allows for the modulation of hydrogel thin-structure controlling molecular weight and mass/volume ratio into the hydrogel precursor solution. Thus, mesh size and porosity can be easily changed as a function of brain ECM morphology and elasticity[16]; contrary to HA which is subject to uncontrollable degradation by cell metalloproteins[17] considerably limiting biological cell studies interpretation, PEG is not susceptible to hydrolytic degradation in comparison to other synthetic polymers non-degradable by cells.[18,19] Therefore, PEG has stable physicochemical properties that allow engineering appropriate biocompatible cell environments to perform more relevant and easier biological cell studies.

Grafting poly-L-lysine (PLL) on the hydrogel was decided because of its ability to promote unspecific cell adhesion. Previously reported PLL-based purely synthetic hydrogels used complex and long term chemical processes for PLL functionalization prior to polymerization.[10] Furthermore, cell adhesion studies that evaluated PLL effects on micro-patterned surfaces used unstable chemical methods to functionalize cell substrates as PLL molecules were only adsorbed to the surface.[20] Other synthesis methods used degradable carbamate crosslinks for PEG–PLL hydrogels polymerization, which resulted in potentially cytotoxic amine degradation byproducts.[21]

In the present work, we investigated the ability of the hydrogel matrix formed by PEG molecules and PLL to modulate, through the variation of the physical characteristics of the matrix, the growth of glioblastoma cell lines. We repeated this study on two different cell lines, the F98 murine tumor cells and the U87-MG human tumor cells. After mild chemical synthesis of a PLL derivative [PLL acrylate (PLL-A)], hydrogels were formed by photopolymerization of a precursor solution containing both PEG-diacrylate (PEG-DA, 6 kDa) and PLL-A (30 kDa). This straightforward technique allowed us to obtain the procurement of a series of matrices of various molecular weights and concentrations in PEG and PLL, capable of sustaining the growth of F98 and U87-MG cells. Based on the results obtained with a cell viability assay (resazurin–resorufin conversion fluorescence technique), a range of various compositions of PEG/PLL (from 3 to 7% PEG, with 0.001 to 0.005% PLL, w/v) containing matrices was analyzed for its physical properties. Hydrogel mesh size and rheological measurements were performed in order to correlate cell growth with the intrinsic gel structure. A significant difference in cell growth was proved between PLL-containing and PLL-free PEG hydrogels, showing the role of non-specific adhesion factors such as PLL in the migration, proliferation and morphological changes induced in both glioblastoma cell lines cultures. Finally, the cytotoxic effect of temozolomide, a drug used in glioma therapy,[22] was assessed on both cell lines F98 and U87-MG on two different substrates, 2D microplate and hydrogels, in order to check for any potential resistance provided by 3D cell organization in aggregates and hydrogel functionality through cell adhesion molecules of PLL.

EXPERIMENTAL

Synthesis of PLL-acrylate

Adapting the method of Ciucurel and Sefton,[23] poly-L-lysine hydrobromide (PLL-HBr 30,000 Da, Sigma-Aldrich, Saint-Quentin Fallavier, France) was dissolved at 1% (w/v) in 50 m*M* bicarbonate buffer solution. The solution was then added to a reaction flask containing acrylic acid succinymidyl ester (169 Da, Sigma-Aldrich, mol ratio 10:1 relative to PLL-HBr dissolved into bicarbonate buffer), and allowed for reacting for 2 h at room temperature under magnetic stirring. The solution progressively changed into milky along with PLL-HBr functionalization. A 5 mL dialysis tubing (MWCO: 0.5–1 kDa; Float-A-Lyzer G2, Spectrum Labs) was first soaked 15 min in deionized water, and then filled with the new PLL-acrylate (PLL-A)

mixture solution. Dialysis against deionized water was carried out during 7 days with daily water change. The extent of PLL-HBr functionalization was quantified by ^{1}H-NMR, on a Brucker DPX250 MHz spectrometer or on a DRX 300 MHz spectrometer using D_2O as deuterated solvent.

Preparation of PLL–PEG Hydrogels for Physicochemical Characterization

Hydrogel precursor solutions were prepared from 3, 5, and 7% (w/v) powder PEG-DA 6 kDa precursor (Sigma-Aldrich), with or without PLL-A, dissolved in [Dulbecco's Phosphate-Buffered Saline (DPBS) buffer without $MgCl_2$ and $NaCl_2$, Gibco], with 0.01% (w/v) of 2,2-dimethoxy-2-phenyl-acetophenone (DMPA; Sigma-Aldrich) solubilized in 1-vinyl-2-pyrrolidone (VP; Sigma-Aldrich). DMPA was used as UV-sensitive photoinitiator, and the concentration was chosen after controlling cell toxicity. Precursor solutions were photopolymerized under UV (UV-LED LC-L1; Hamamatsu, $\lambda = 365$ nm, 2 W/cm^2) for 40 s in homemade cylindrical dishes. Photopolymerized hydrogels were then incubated during 1 day in a high volume of DPBS for the hydrogel structure to be hydrated and thermodynamically stable before characterization.

Raman Spectroscopy Analysis

Raman spectra were obtained as in Hui-Bon-Hoa *et al.*,[24] with a home-built near-infrared (NIR) Raman setup. Raman excitation at 780 nm (about 100 mW) was provided by continuous-wave Ti:Sapphire laser (Spectra Physics model 3900S) pumped by Ar-ion laser (Spectra Physics Stability 2017). Rayleigh-scattered light was filtered off with a pair of dichroic beam splitter plus long-pass filter (Semrock RazorEdge). Raman scattering was excited using either a long working distance air objective (Olympus 10X, NA = 0.25) for dry samples or a water-immersion objective (Olympus LUMFL, 60X, NA = 1.1) for solutions and hydrated gels. Raman light was collected in backscattering geometry, dispersed by 500-mm focal length spectrograph (Acton SpectraPro 2500i) with a slit width set to 40 µm, and registered by a deep-depletion back-illuminated NIR CCD detector (Princeton Instruments SPEC-10 400BR/LN), cooled down to 140 K by liquid nitrogen. The spectral resolution was ~4 cm^{-1}. Hydrogel samples were prepared as described above and were not dried before measurements. The relative number of C=C bonds in the gels (present in the acrylate function), used as a measure of the degree of crosslinking, was obtained by comparison of the respective Raman band intensities attributed to C=C stretching at different PEG-DA concentrations (band frequency at 1640 cm^{-1} in water solution shifts to 1644 cm^{-1} in PEG-DA gels).

Mesh Size Calculation

When polymeric chains are crosslinked and swollen in a thermodynamically good solvent (polymer–solvent interactions are favored compared to polymer–polymer interactions), polymer macromolecules attain an open structure, a solvated state that maximize polymer–solvent contacts and minimize polymer chains interactions.[25] The global effective volume of the gel increases as polymer–solvent interactions swell the global structure of the gel. A characteristic correlation length can be defined as the average distance between two consecutive crosslinks. This correlation length is called the mesh size of the polymer network.[26] The mesh size indicates the maximum size of solutes that can pass through this network, and serves as an indicator of the screening effect of the polymer network, on solute diffusion within the swollen hydrogel.

For a primary approach of hydrogels permeability, a range of 6 kDa PEG-DA hydrogels at three different polymer concentrations [3, 5, and 7% (w/v)] and fixed photoinitiator concentration [0.01% (w/v) DMPA in VP solvent] was probed.

Flory–Rehner calculations modified by Peppas and Merrill were used to determine hydrogel mesh size (ξ).[27] The hydrogel weight was recorded after 24 h incubation with DPBS for equilibrium swelling, and subsequently after drying in a stove at 60 °C for 48 h and under vacuum for 4 h.

First, the estimated molecular weight between crosslinks (M_c) was calculated with eq. (1).

$$\frac{1}{M_C} = \frac{2}{M_n} - \frac{\bar{\nu}\left[\ln(1-\nu_{2,s}) + \nu_{2,s} + \chi\nu_{2,s}^2\right]/V_1}{\nu_{2,r}\left[\left(\frac{\nu_{2,s}}{\nu_{2,r}}\right)^{1/3} - \frac{1}{2}\frac{\nu_{2,s}}{\nu_{2,r}}\right]} \quad (1)$$

Flory–Rehner equation modified by Peppas and Merrill[27] for the calculation of average molecular weight between crosslinks (M_c) where M_n is the polymer average molecular weight before crosslinking; V_1 is the molar volume of the water solvent (18 cm^3 mol^{-1}); $\nu_{2,s}$ is the polymer volume fraction of the swollen hydrogel when the hydrogel is fully swollen defined as $\nu_{2,s} = 1 + \frac{\rho p}{\rho s}\left(\frac{M_r}{M_d} - 1\right)$, $\nu_{2,r}$ is the polymer volume fraction of the hydrogel immediately after crosslinking and before any additional swelling defined as $\nu_{2,r} = 1 + \frac{\rho p}{\rho s}\left(\frac{M_r}{M_d} - 1\right)$, with ρ_p the density of the dry hydrogel before crosslinking (1.12 g/cm^3 for PEG), ρ_S the density of the solvent (1.01 g/cm^3 for DPBS), M_r the hydrogel mass just after crosslinking before swelling, M_s the hydrogel mass after swelling, and M_d the hydrogel mass after drying process; $\bar{\nu}$ is the specific volume of the PEG polymer (0.893 cm^3 g^{-1}, $1/\rho_p$) and χ is the Flory–Huggins polymer–solvent interaction parameter (0.426 for PEG–water assumed constant during experiments as determined by Griffith and Lopina.[28]

Mesh size was then determined as described by Canal and Peppas[26]; the root-mean-square end-to-end distance of the polymer chain in the unperturbed state $(\bar{r}_0^2)^{1/2}$ was calculated using eq. (2).

$$(\bar{r}_0^2)^{1/2} = l C_n^{1/2}\left(2\frac{M_c}{M_r}\right)^{1/2} \quad (2)$$

Expression of the root-mean-square end-to-end distance of the polymer chain in the unperturbed state (solvent-free) $(\bar{r}_0^2)^{1/2}$ where l is the average bond length (0.146 nm), C_n is the characteristic ratio of the polymer (typically 4.0 for PEG), M_c is the average molecular weight between crosslinks, and M_r is the molecular weight of the PEG unit (44 g mol^{-1}).

Mesh size was finally calculated from eq. (3).

$$\xi = (\bar{r}_0^2)^{1/2}\nu_{2,s}{}^{-1/3} \quad (3)$$

Mesh size equation where $(\bar{r}_0^2)^{1/2}$ is the root-mean-square end-to-end distance of the polymer chain in the unperturbed state (solvent-free) and $\nu_{2,s}$ is the polymer volume fraction of the swollen hydrogel at equilibrium.

Rheology: Small-Amplitude Oscillatory Shear Experiments

The rheological properties of hydrogels were evaluated by oscillatory shear experiments. The tests were performed using a controlled-stress rheometer (AR-G2, TA instruments, Guyancourt, France) equipped with a parallel-plate geometry (8 mm diameter). The instrument was preheated at 25 °C to reach the temperature of the operating room and maintained to this value throughout the test. The gap was fixed at 500 µm. To determine the hydrogel gelation time, dynamic strain sweeps were performed at a frequency of 1 Hz with a strain amplitude ranging from 0.01 to 8000%, after different UV-irradiation times ranging from 0 up to 8 min. Elastic modulus G' and viscous modulus G'' were determined in the linear regime at 1% strain. Results are based on three repetitions for each sample condition.

Glioma Cell Lines and Chemicals

Glioma cell lines of F98 from rat model and U87-MG from human glioma were provided by ATCC (CRL 2397 and HTB-14, respectively). Cells were maintained in Dulbecco's Modified Eagle's Medium (DMEM; Life Technologies, Courtaboeuf, France) added with phenol red as pH indicator, supplemented with 4.5 g/L of D-glucose and pyruvate, 10% (v/v) fetal bovine serum (Life Technologies), and 1% (v/v) of penicillin and streptomycin antibiotics (Pen-Strep, Life Technologies). Cells were disposed into sterile culture flasks with anti-fungal filters to limit contamination and maintained in culture at 37 °C, under a humidified atmosphere of 95% relative humidity with 5% CO_2. Cells were replicated when they attained 80–90% cell confluence. Cell splitting periodicity was established to twice a week with 0.05% trypsin (trypsin-EDTA 1X, Life Technologies), as cell proliferation was estimated to 2×10^6 cells/day for F98 cell line and 4×10^5 cells/day for U87-MG cell line in culture flasks. For temozolomide effect assessment, the drug was purchased from Sigma-Aldrich and a 25 m*M* stock-solution was prepared in DMSO prior to use.

Hydrogels Preparation and *In Vitro* Cell Culture

Hydrogels were prepared from 3% (w/v) PEG-DA 6 kDa precursor (Sigma-Aldrich), dissolved in DPBS with 0.01% (w/v) of DMPA solubilized in VP. Precursor solutions were photo-polymerized under UV (UV-LED LC-L1; Hamamatsu, 2 W/cm^2, $\lambda = 365$ nm) for up to 60 s depending of the experiment in 48-well sterile Corning microplates. Photo-polymerized hydrogels were then incubated during 1 day in a high volume of DMEM for the hydrogel structure to be hydrated and thermodynamically stable before cell seeding. After this day of hydration and two rinsing with fresh medium, cells were seeded upon hydrogels at 2×10^5 cells/well. To avoid cell medium acidification, cell culture medium was replaced by fresh medium every day.

Quantification of Cell Viability and Proliferation: Resazurin Assay

For assessing cell viability and proliferation in 2D conditions, both F98 and U87-MG cell lines were seeded at the definite amount of 10^4 cells/well. Cell viability was initially assessed 2 h after cell plating, and then followed during 5 days, using the standard fluorimetric resazurin assay.[29] Resazurin is metabolized by mitochondrial redox coenzymes of living cells; the oxidation product of colorless resazurin, resorufin, is fluorescent and easily quantified as proportional to the relative number of living cells. Cell fluorescence was detected with a microplate reader (Fluoroskan Ascent Thermo Scientific microplate reader) exciting at 530–570 nm and collecting the resorufin signal at 590–620 nm. For quantifying F98 and U87-MG viability, 239 µM of resazurin (resazurin sodium salt, Sigma-Aldrich) dissolved into DMEM and filtered was added to each well [0.006% (w/v)]. After 2 h of incubation at 37 °C, 5% CO_2, 95% relative humidity, cell viability was read. The calibration between cell viability percentage and effective cell number was done on 2D experiments and hydrogels for both cell lines. This method allows assessing the relative metabolism differences between cell lines. The same protocol was followed for quantifying F98 and U87-MG cell viability and proliferation on hydrogels based on Mahoney and Anseth.[30]

Quantification of Cell Growth on Hydrogels: Microscopy and Image Processing

Microscopy image acquisition was performed using a 10X Nikon water-immersion objective placed on an Eclipse 80i Nikon microscope (Scop Pro, Marolles-en-Hurepoix, France), which is equipped with a complete enclosure allowing for the fine control of temperature, humidity and CO_2 pressure on the living sample (Box and Cube system by Life Imaging Services, Basel, Switzerland). Micrographs series were obtained using a Zyla 5.5 MPX Andor SCMOS cooled camera (Scop Pro, France) and MetaMorph acquisition software (Molecular Devices, Sunnyvale, CA).

Image processing was performed with Fiji analysis software to quantify areas and density of cell aggregates. Customized Fiji macro files were developed to analyze the data as follows: since only the global shape of aggregates and the number of aggregates per surface unit are relevant, the information to extract from individual cells in the image processing boiled down to the area of aggregates and the number of aggregates. Therefore, the images were smoothed out through multiple Gaussian blurry filters. Then edge detection was applied to select cell aggregates thanks to the intensity contrast between the inside and the outside of the aggregates. Finally, an in-house customized macro calculated the area of the delimited objects and their number. Only objects with an area larger than the area of one cell were kept for analysis to exclude isolated cells.

RESULTS AND DISCUSSION

Synthesis of PLL-A

The acrylic acid *N*-hydroxy succinimidyl ester was used to add acrylate groups to PLL and the number of acrylate groups per PLL was estimated by ^{1}H-NMR (Figure 1). The values of the integrals for the vinyl protons (5.7–6.5 ppm, 3 protons per acrylate group added) and for the beta, gamma and sigma protons on the PLL chain (1.2–1.8 ppm, 6 protons per lysine residue) were used to calculate the degree of substitution. With a typical reagent ratio 1:10 (PLL-HBr 30 kDa/*N*-hydroxysuccinimide acrylate) and a reaction time of 2 h, the ratio of the integrals for the lysine/acrylate protons was found to be 119.4/3.2. In the case of a substitution degree of one lysine residue per one acrylate group, the proton ratio would be 6/3. In our case, we then had one acrylate per 18.7 lysine residue. Since the PLL 30 kD is composed of around 200 lysine residues, the degree of substitution was 10.7 acrylate group per PLL molecule; in excess, as expected.

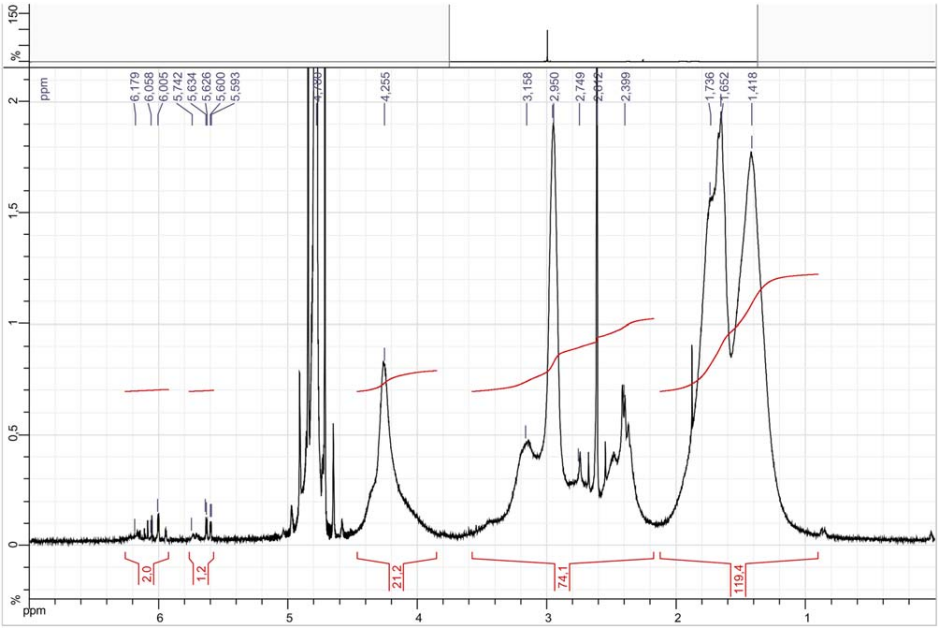

Figure 1. ^{1}H-NMR spectrum of the 30 kDa PLL-acrylate derivative. [Color figure can be viewed at wileyonlinelibrary.com]

Raman Spectroscopy Analysis

In order to analyze the crosslinking degree and the possible chemical mechanism of photopolymerization, we studied by Raman spectroscopy (RS) samples of variable composition in PEG-DA 6 kDa without and with PLL-A monomers (so-called "inert" and "adhesive" materials) at a concentration of 0.01% (w/v). We compared the intensities of Raman peak at 1644 cm^{-1} assigned to C═C bonds stretching, which is only in the PEG-DA monomer. Through an addition-reaction during polymerization, the diacrylate groups were replaced by simple covalent bonds between two ends of PEG molecules. Then, the number of C═C bonds, and therefore the 1644 cm^{-1} RS peak, could be used as a measure of the degree of crosslinking of the polymer meshwork. To follow the C═C bond reaction we analyzed how RS signature of the hydrogel changes with PEG-DA and PLL-A concentrations. First of all, the PLL-A 0.01% concentration, while higher than the one used to study cell proliferation, was not high enough to be distinguishable by RS or to modify the spectra of PEG-DA alone. Looking only at PEG-DA photopolymerization, the intensity of Raman peak at 1644 cm^{-1} decreased in intensity as PEG-DA concentration increased (Figure 2). Integrated intensity of the C═C band within the range 1600–1690 cm^{-1} showed a sharp decrease with increasing PEG-DA concentration until reaching a plateau after 5% (w/v) PEG-DA concentration. Below 2.5% (w/v) PEG-DA concentration, there was no photopolymerization-related phase transition between solution and hydrogel. Starting at 2.5% (w/v) PEG-DA concentration, the gel structure is very loose and most of the original C═C monomeric bonds are not involved in the polymer bond. At 3% (w/v) and higher, the density of monomer molecules leads to the formation of a more dense and stiff hydrogel network.

Mesh Size

The mesh size was calculated for both inert and adhesive hydrogels to check both PEG concentration and PLL addition effects on hydrogels architecture. Swelling studies were performed for three concentrations of PEG-DA 6 kDa hydrogels with different putative cell adhesive properties: "less" and "more" adhesive

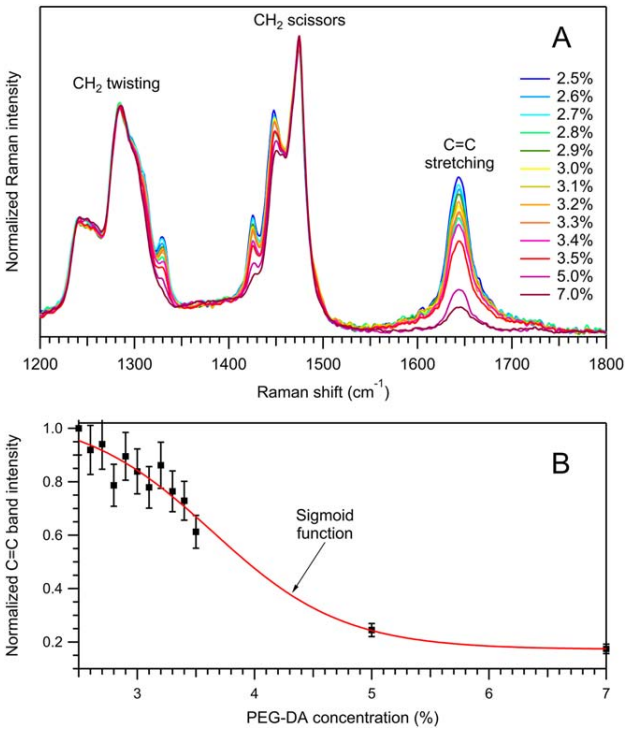

Figure 2. (a) Raman spectral fingerprints of PEG-DA hydrogels recorded at various hydrogels concentrations probed. Raman spectra were normalized on H—C—H deformation modes at 1285 (CH_2 twisting) and 1475 cm^{-1} (CH_2 scissors). (b) Normalized C═C band intensity integrated within 1600–1690 cm^{-1} range as a function of PEG-DA concentration. [Color figure can be viewed at wileyonlinelibrary.com]

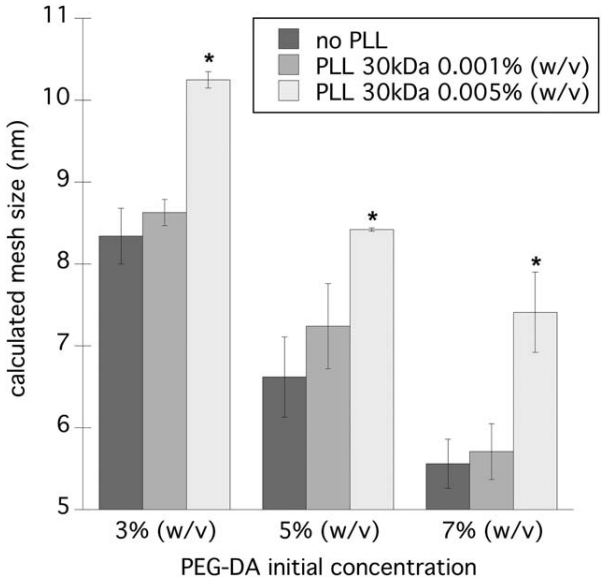

Figure 3. Mesh size calculations for three hydrogel formulations with different adhesive properties ($n = 3$ for each formulation). $^*P < 0.05$ versus PEG-DA concentrations (3, 5, and 7%) with no PLL.

hydrogels with, respectively, low [0.001% (w/v)] and high concentration [0.005% (w/v)] of PLL-A 30 kDa. The range of mesh size values covered by all hydrogels is small with values ranging from ~5 to 10 nm (Figure 3). Results showed that PEG-DA concentration is the main parameter that controls hydrogel mesh size. A linear decrease of mesh size with increasing PEG-DA concentration was found. Addition of PLL-A 30 kDa resulted in higher mesh size values because PLL-A molecule blocks the polymerization process between two PEG-DA molecules, thus increasing the distance between reticulation points.

Mechanical Properties

Hydrogel structure and PEG-DA concentration range probed for this experiment were first assessed using irradiated precursor solutions at different UV-irradiation times. Low monomer PEG-DA 6 kDa concentration of 3% (w/v) was used to evaluate hydrogel gelation time. Elastic modulus (G') and viscous modulus (G'') were quantified at different UV irradiation times (from 0 to 8 min) (Figure 4). Results showed a fast increase in G' and G'' values that reach a plateau at 1 min UV. Complete gelation occurred around 1 min of UV irradiation. Hydrogels precursor solutions that polymerized were predominantly elastic from 30 s up to 8 min UV-irradiation time as $\tan \delta = 0.04$ for this time range (with δ the phase angle and $\tan \delta = G''/G'$). Thus, after complete gelation, the elastic modulus G' best characterized the mechanical properties of the hydrogels. Elastic modulus G' values were taken after a 6 min UV-irradiation time to ensure complete gelation for all PEG-DA 6 kDa hydrogel concentrations probed.

As for mesh size calculations, the same range of PEG-DA 6 kDa concentrations and formulations (with or without PLL-A, at two different concentrations) were probed. A linear increase of G' was observed with increasing PEG-DA concentration for PLL-A-based hydrogels (Figure 5). When the PEG-DA

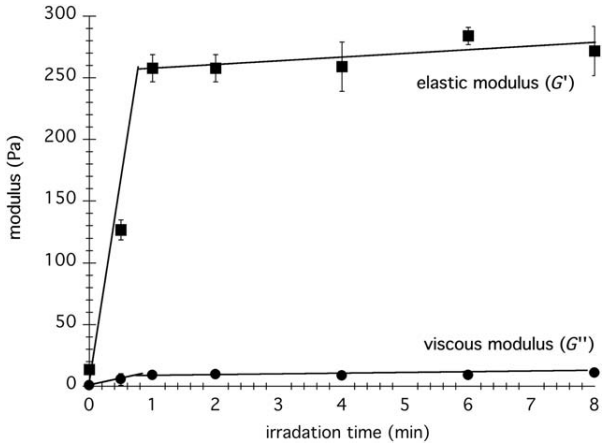

Figure 4. Time course of the photopolymerization of a PEG-DA 6KDa 3% w/v precursor solution, showing G' (elastic contribution) and G'' (viscous contribution) moduli versus UV ($\lambda = 365$ nm) irradiation times.

concentration was divided by around two [lowered from 7 to 3% (w/v)], hydrogels exhibited lower stiffness values with a 20-times smaller elastic modulus around 300 Pa. PLL-A-based formulations exhibited slightly higher stiffness than inert hydrogels but no significant difference were found between both PLL-A concentrations. Interestingly, the increased stiffness observed with PLL-A could be correlated with the increased mesh size. Even if it would seem counterintuitive, it is probably related to the fact that the additional PLL-A polymerization inside the hydrogel PEG bulk is due to the replacement of a PEG-DA molecule by a larger PLL-A molecule, expelling the water out of this small domain.

Cell Viability

As a primary approach of hydrogel biocompatibility, cell viability was quantified on hydrogels over a range of PEG-DA 6 kDa

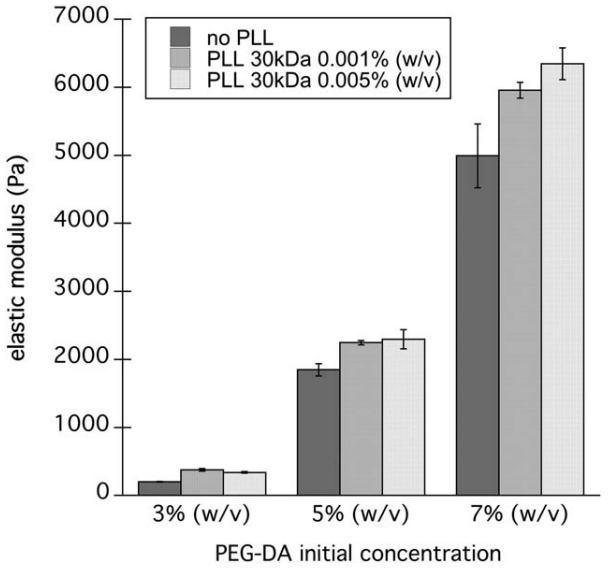

Figure 5. Elastic modulus representing mechanical properties of different hydrogel formulations (PEG-DA 6 kDa, with or without PLL-A 30 kDa) with variable adhesive properties ($n = 3$ for each hydrogel condition).

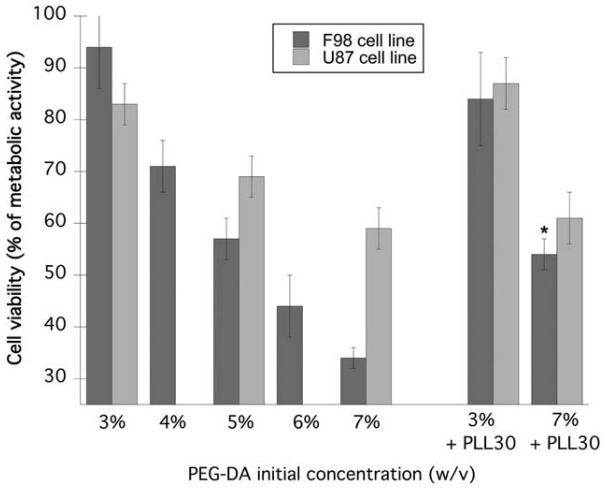

Figure 6. Cell viability for various PEG-DA 6 kDa concentrations and with PLL-A 30 kDa addition for F98 and U87-MG glioma cell lines. Results are expressed relatively to those obtained from 3D-matrigel substrate on which cells were seeded at the same density ($n = 3$ independent experiments for each condition). $^*P < 0.05$ versus F98 cell line grown on 7% PEG-DA with no PLL, considering each cell line and between each PEG-DA concentration, $^*P < 0.05$.

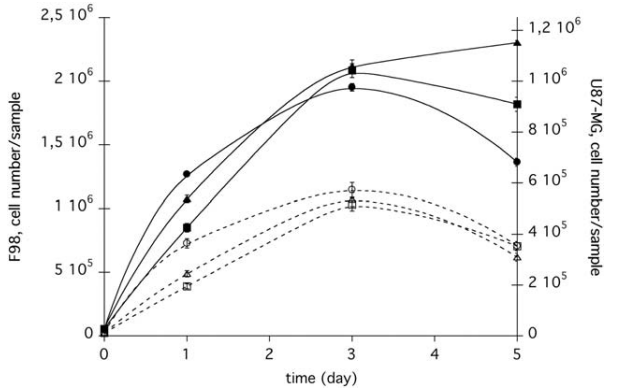

Figure 7. F98 (solid lines) and U87-MG (dashed lines) cell numbers over 5 days of cell culture on hydrogels with different adhesive properties: no PLL (inert, circles), PLL30 0.001% (w/v) (lower cell adhesion, squares) and PLL30 0.005% (w/v) (higher cell adhesion, triangles). Results are expressed from three samples for each hydrogel condition at each time point.

concentrations for both cell lines after 5 days of cell culture. Cell viability of U87-MG and F98 cell lines was considerably impeded by increasing hydrogel stiffness (i.e., PEG concentration) (Figure 6). Whereas the mean cell survival rate of F98 cells was 90% on soft hydrogels [3% (w/v)], six-times more F98 cells died on stiff substrates [7% (w/v)]. U87-MG cells were less affected by hydrogel stiffness: the mean cell survival was 60% on stiff substrates and 70% on soft substrates.

Further experiments were done to assess a potential cytotoxic effect upon PLL-A addition. As a preliminary experiment, PLL-A solutions were first added to preformed PEG-DA hydrogels without concomitant photopolymerization and the resulting hydrogel was compared to PEG-only hydrogels for cell viability: in this case, there was no significant difference between both conditions (data not shown). When the hydrogel was formed by polymerization of PEG-DA and PLL-A together, a decrease in cell viability was also observed for the increased PEG-DA concentrations. However, in the presence of PLL-A, different trends were observed depending on the cell line considered. Indeed, with soft hydrogels, addition of high-concentrated PLL-A 30 kDa [0.005% w/v] seemed slightly cytotoxic for F98 cells, whereas no significant effect was found on U87-MG cell proliferation. On stiff hydrogels, addition of PLL-A with a high concentration promoted F98 cell survival with a significant gain in cell viability, as twice more cells survived when they were attached to the substrate. This was not the case for U87-MG cells for which cell survival percentage stayed the same whether they were on the inert hydrogel or on the adhesive one.

Cell Proliferation

Because of better cell viability results on soft hydrogels, a subset of formulations corresponding to 3% (w/v) PEG-DA-based hydrogels, inert and adhesives was finally chosen for *in vitro* cell studies. These conditions are summarized in Table I. Are also reported the apparent cell adherence behavior, the calculated PLL surface density, as well as the calculated mesh density (using the measured mesh size values). Resazurin tests (cytotoxicity assays) were performed over 5 days to quantify cell growth on different hydrogels formulations.

According to the cell type, the growing behavior was different. For both cell lines, a common increase was observed for all hydrogel formulations over the first 3 days of culture (Figure 7), up to 2×10^6 cells/sample for the F98 line but to a less extent for U87-MG cells with an average value of 10^6 cells/sample. Beyond day 3, a common decrease more or less important in cell number was observed among cell lines between inert and less adhesive hydrogels: F98 cell number drops to 7×10^5 cells/sample for inert hydrogels and to 9×10^5 cells/sample for less adhesive hydrogels; whereas U87-MG drops to a lower value to 3.5×10^5 cells/sample for all hydrogel formulations. On the contrary, this drop in cell number was not observed for F98

Table I. Hydrogel Conditions Tested for In Vitro Cell Culture

Hydrogel type	PEG 6kDa 3% (w/v) No PLL	PEG 6kDa 3% (w/v) + PLL30 kDa 0.001% (w/v)	PEG 6kDa 3% (w/v) + PLL30 kDa 0.005% (w/v)
Cell adherence	none	low	high
Calculated PLL surface density (ng/mm^2)	—	0.016	0.08
Measured mesh density (10^3 mm^{-2})[a]	14.4 ± 4.8	13.4 ± 2.1	9.5 ± 0.9

[a] Measured mesh size is considered as the side of a square, allowing to calculate the mesh area, and therefore the mesh density.

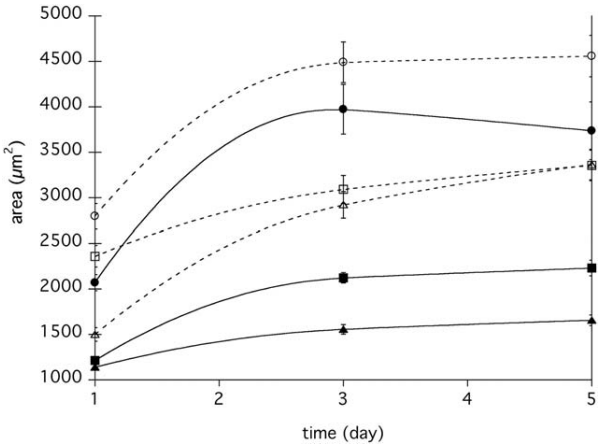

Figure 8. Time courses of F98 (solid lines) and U87-MG cell lines (dashed lines) aggregate area on hydrogels with different adhesive properties: inert (circles), PLL 30 kDa 0.001% (w/v) (lower cell adhesion, squares), PLL 30 kDa 0.005% (w/v) (higher cell adhesion, triangles) ($n = 8$ for each hydrogel condition).

cells on more adhesive hydrogels for which the mean cell number seemed to continuously increases but more slowly than on other hydrogels. Thus adhesive hydrogel seemed to enhance F98 cell survival over long-term cell culture but no effect of hydrogel adhesion was seen on U87-MG cell viability over 5 days.

Cell Aggregates Formation

As for proliferation assays, cell growth was also quantified over the same period of time taking micrographs of cultures on days 1, 3, and 5. At day 1, both cell lines were organized in cell aggregates growing on very soft hydrogels (around 300 Pa). Using as quantitative indicators the projected area of cell aggregates and aggregates density over time, cell growth was quantified on different hydrogel formulations. For each cell line, aggregates areas were significantly different between inert hydrogel (no PLL) and adhesive hydrogels (PLL 30 kDa). This observation was strengthened by the difference in cell aggregates densities observed for each formulation of the hydrogel. Indeed, for inert hydrogels, cell aggregates were less numerous but bigger, of the order of 60 aggregates/mm^2 with a mean area of 3500 μm^2 in average, for both cell lines, whereas for adhesive hydrogels, cell aggregates were more numerous but much smaller, of the order of 100 aggregates/mm^2 with a mean area of 2200 μm^2 in average, for both cell lines.

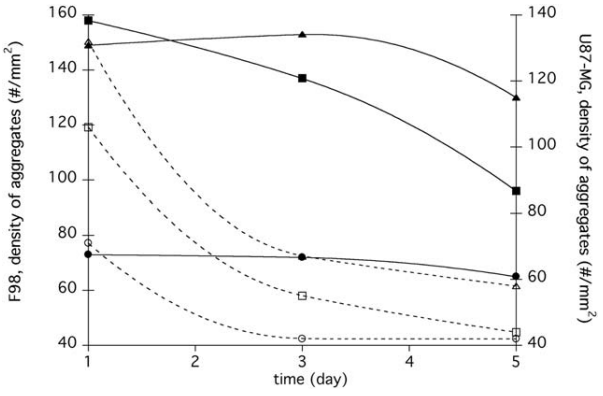

Figure 9. Time courses of F98 (solid lines) and U87-MG cell lines (dashed lines) aggregate density on hydrogels with different adhesive properties: inert (circles), PLL 30 kDa 0.001% (w/v) (lower cell adhesion, squares), PLL 30 kDa 0.005% (w/v) (higher cell adhesion, triangles) ($n = 8$ for each hydrogel condition).

Considering F98 cell line, aggregate areas increased over 5 days (Figure 8, solid lines), although their density remained stable [Figure 9, solid lines)]. Thus, the increase was only due to cell proliferation in aggregates. In addition, the more adhesive was the hydrogel, the slower was the cell growth (Figure 10).

The number of aggregates of U87-MG cells per surface unit decreased for all hydrogel formulations progressively. This decrease of the density of cell aggregates was observed as cells proliferated (detected aggregates were bigger over time), which led to fusion of aggregates (Figures 8 and 9, dashed lines; Figure 11).

Evaluation of Temozolomide Effect on Cell Growth

The effect of temozolomide, was assessed on both cell lines F98 and U87-MG on two different substrates, 2D regular Petri dishes and the present PEG-PLL hydrogels.

By submitting F98 and U87-MG cells plated in 2D to a range of drug concentrations from 100 to 2000 μM and measuring the cell viability after 20 h exposure, the median inhibition concentration IC_{50} was calculated for both cell lines at 455 ± 24 μM. The determined value of IC_{50} in 2D was then used to check cell viability on hydrogels. Results (Figure 12) showed that for both cell lines, a smaller fraction of cells died compared to 2D: on hydrogels, the final numbers of cells (respectively F98 and U87-MG) were 30 and 20% smaller than in absence of the drug, whereas the final numbers of cells were 65 and 50% smaller on Petri dishes. In detail, U87-MG cells revealed being globally more resistant to the drug than F98 cells: cell viability on hydrogels of U87-MG cells was around 7–10% higher than viability of F98 cells, whereas U87-MG cell viability was 30% higher than for the one of F98 cells in 2D. PLL addition however did not improve the cell viability on the PEG only hydrogel, while maintaining a higher cell resistance than in 2D. Furthermore, PLL seemed to decrease the beneficial effect of growth on hydrogel versus 2D, maybe because of an additional synergic toxicity between PLL and temozolomide.

CONCLUSIONS

In the present work, we fabricated and characterized hydrogel scaffolds based on poly(ethylene glycol) and PLL to support glioma cell culture and eventually study *in vitro* tumor cell growth in response to extracellular physicochemical changes over the time-course of 5 days. Manufacturing a minimalistic hydrogel, with only three affordable reagents (PEG-DA, PLL-A, and DMPA), we were able to create hydrogel structures under mild chemical conditions using a straightforward photo-polymerization technique. In these conditions, we could recreate pseudo-3D microtumor-like cell systems with physiological organization such as those found in Matrigel.[31]

The parameters tested to characterize the physicochemical properties of the hydrogels (i.e., elastic modulus and mesh size) matched referenced values in the literature for PEG-DA-based hydrogels

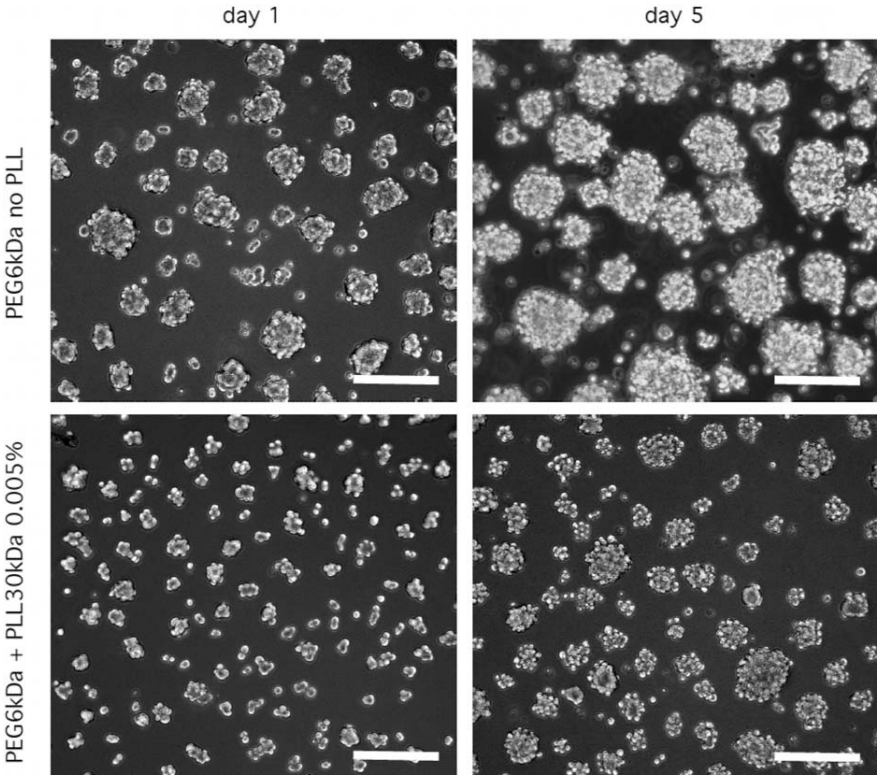

Figure 10. Time-lapse of F98 cell aggregates on hydrogels with different adhesive properties over 5 days. Scale bar = 50 μm.

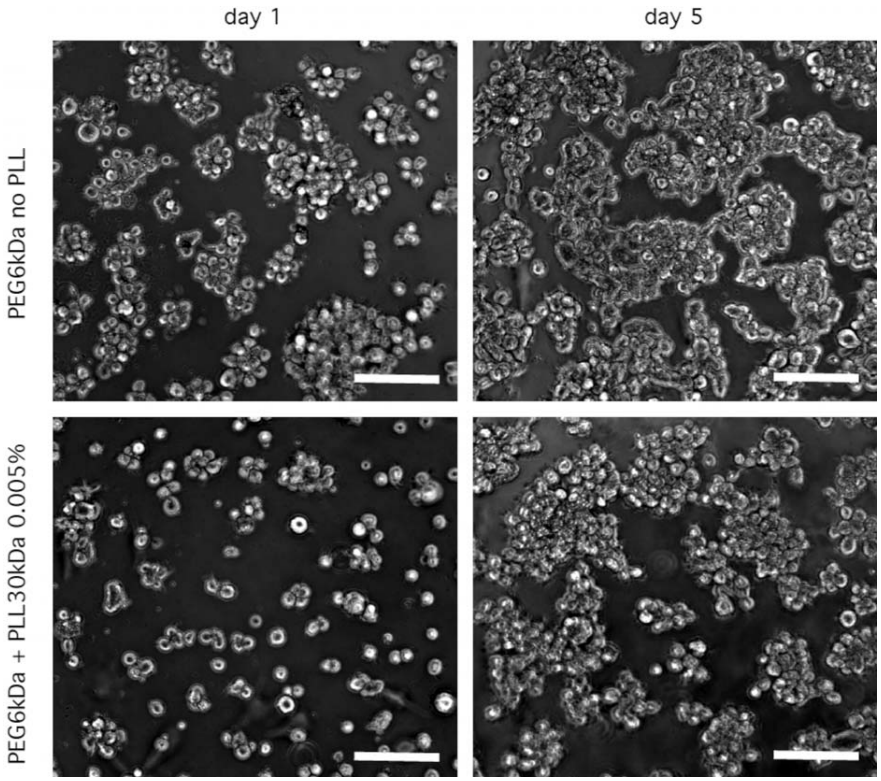

Figure 11. Time-lapse of U87-MG cell aggregates on hydrogels with different adhesive properties over 5 days. Scale bar = 50 μm.

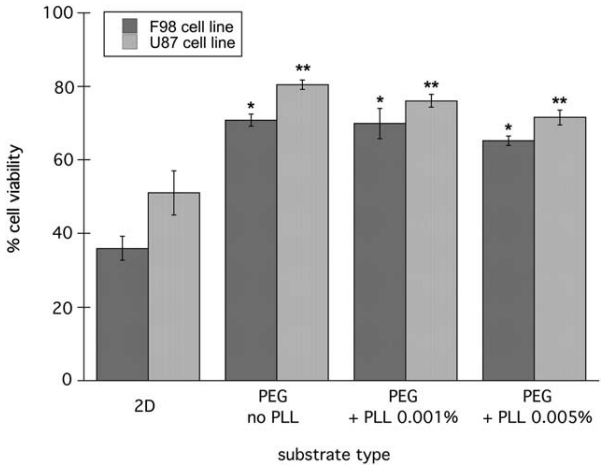

Figure 12. Effect of temozolomide on cell viability of F98 and U87-MG cells lines. Cells plated on Petri dish or PEG hydrogel with or without PLL were assayed after a 20 h treatment with 455 μM temozolomide and 3 days of culture ($n = 3$). *$P < 0.05$ versus 2D growth condition for F98 cell line; **$P < 0.05$ versus 2D growth condition for U87-MG cell line.

synthetized by other chemical reaction processes.[30,32–34] This validated the simpler and affordable process suggested here. Modulating hydrogel components resulted in more or less pronounced effects on hydrogel properties: in particular, raising PEG-DA concentration resulted in increased hydrogel crosslinking, a concomitant higher mechanical strength, and a lower mesh size. The addition of PLL-A had a slightly limited effect on both mechanical and mesh size features: mesh size was finely tuned with addition of PLL-A incorporated into the PEG backbone and stopping the polymerization process, thus resulting in larger voids into the polymeric network and a bigger general mesh size.

In reaction to these differences between physicochemical properties, cells exhibited different growth and organization patterns. Rounded cell shape and cell organization were consistent over all hydrogel formulations probed and both glioma cell lines. However, the modulation of the hydrogel composition and physicochemical properties tuned the cell growth pattern. Indeed, cell viability was higher on softer hydrogels scaffolds [245 Pa in average for 3% (w/v) formulations] with lower mechanical strength to cell strains, in comparison to stiff hydrogels [5 kPa for 7% (w/v) formulations]. These results are consistent with glioblastoma cells and neural stem cells viability on soft hydrogels.[10,35] We hypothesized that cell viability, morphology, and organization are due to concomitant effect of hydrogel stiffness, low substrate affinity, and strong intercellular junctions. On soft substrates, cell viability may be increased by deformability of the underneath polymeric network. When cell divisions occur or when cell reorganize, strong intercellular junctions, and cell–hydrogel interactions are involved into the 3D structure of aggregates. Thus, deformability of the substrate may be crucial to support cell viability and growth.[36]

Functionalization of hydrogels with PLL had a very slight impact on hydrogel physical properties, compared to PEG only. The main effect was observed in mesh size calculations, with increasing values of the typical mesh dimension, whereas cell aggregates were smaller and more numerous. We hypothesized that PLL molecules filled the voids left by the polymerization process, creating many local adhesion sites at the surface of the hydrogel that support cell growth of aggregates (see Table I for PLL surface density estimation). Moreover, with cell viability results, we showed that each cell line presents different susceptibilities to hydrogel functionalization with PLL. Thus, with a range of PLL-A concentrations considered as toxic in solution,[37,38] we showed that increasing PLL-A concentration to modulate cell adhesion on the hydrogel is possible in the range 10–30 μg/mL. Above this value, PLL-A is significantly toxic for the cells. By modulating cell growth, cell adhesion favored cell viability while limiting aggregate sizes. Limited sizes of cell aggregates may potentially impact individual cell viability, by favoring diffusion of nutrients throughout cells from a same aggregate.[39]

Finally, our hydrogel substrate facilitated cell growth analyses over time due to surface cell repartition and stable physicochemical properties. This shall be particularly interesting to quantify cell dynamics (proliferation, growth) at the surface of the hydrogel, whereas it is more difficult with degradable hydrogels whose physical properties are more difficult to tune. Because of its simplicity, affordability and easy use, this substrate could also be used for *in vitro* drug screening in conditions closer to the *in vivo* 3D cell arrangement in tissues, even if the cells are not growing inside the hydrogel but on top of it. As an illustration, we have shown that the drug temozolomide has a differential effect on 2D versus 3D cell organization. Finally, beside the use of this type of gel to grow other cell types, the versatile polymerization technique through a simple acrylated molecule added altogether with the PEG-DA in the precursor solution, should probably allow for the addition of other functionalized peptides. As a good candidate, the Arg-Gly-Asp (RGD) tripeptide is the minimal motive of the fibronectin protein that promotes cell adhesion through specific recognition by cell adhesion proteins called integrins[40,41]; it could probably be grafted to PEG monomers with similar method as such used in our study. However, the comparative RGD/PEG molecular weight ratio would probably need the RGD molecules to be made longer with linker molecules helping for RGD conjugation to PEG-DA monomers.[42]

ACKNOWLEDGMENTS

The authors would like to thank Katell Sénéchal-David (ICMMO, Orsay, France) for her special assistance in performing the RMN analysis. This work was supported through a grant from Région Île-de-France ("DIM Problématique transversales aux systèmes complexes" ISC-2014-PME-003) and a grant from the GEFLUC (Groupement des Entreprises Françaises dans la Lutte contre le Cancer) society. E. Gontran was awarded a 3-year doctoral fellowship from the Paris-Saclay Idex.

REFERENCES

1. Louis, D. N.; Ohgaki, H.; Wiestler, O. D.; Cavenee, W. K.; Burger, P. C.; Jouvet, A.; Scheithauer, B. W.; Kleihues, P. *Acta Neuropathol.* **2007**, *114*, 97.

2. Bolteus, A. J.; Berens, M. E.; Pilkington, G. *J. Curr. Neurol. Neurosci. Rep.* **2001**, *1*, 225.
3. Janmey, P. A.; Miller, R. T. *J. Cell Sci.* **2011**, *124*, 9.
4. Tibbitt, M. W.; Anseth, K. S. *Biotech. Bioeng.* **2009**, *103*, 655.
5. Zhu, J.; Marchant, R. E. *Expert Rev. Med. Dev.* **2011**, *8*, 607.
6. Georges, P. C.; Miller, W. J.; Meaney, D. F.; Sawyer, E. S.; Janmey, P. A. *Biophys. J.* **2006**, *90*, 3012.
7. Wang, T. W.; Spector, M. *Acta Biomater.* **2009**, *5*, 2371.
8. Hoffman, A. S. *Adv. Drug Deliv. Rev.* **2012**, *64*, 18.
9. Pedron, S.; Becka, E.; Harley, B. A. C. *Biomaterials* **2013**, *34*, 7408.
10. Wang, C.; Tong, X.; Yang, F. *Mol. Pharm.* **2014**, *11*, 2115.
11. Ananthanarayanan, B.; Kim, Y.; Kumar, S. *Biomaterials* **2011**, *32*, 7913.
12. Oh, Y.; Cha, J.; Kang, S.-G.; Kim, P. *J. Ind. Eng. Chem.* **2016**, *39*, 10.
13. Isayeva, I.; Das, S. S.; Chang, A.; DeFoe, J.; Luu, H.-M.; Vorvolakos, K.; Patwardhan, D.; Whang, J.; Pollack, S. *J. Biomed. Mater. Res. Part B: Appl. Biomater.* **2010**, *95B*, 9.
14. Lee, S.; Tong, X.; Yang, F. *Acta Biomater.* **2014**, *10*, 4167.
15. Discher, D. E.; Janmey, P.; Wang, Y.-L. *Science* **2005**, *310*, 1139.
16. Raic, A.; Rödling, L.; Kalbacher, H.; Thedieck, C. L. *Biomaterials* **2014**, *35*, 929.
17. Wiranoswska, M.; Rojiani, M. V. In Glioma Progression, Glioma: Exploring Its Biology and Practical Relevance, Ghosh, A., Ed.; InTech; **2011**, Chapter 12, p 257.
18. Principles of Regenerative Medicine; Atala, A.; Lanza, R., Thomson, J. A., Nerem, R.; Eds. Academic Press: San Diego, **2010**.
19. Browning, M. B.; Cereceres, S. N.; Luong, P. T.; Cosgriff-Hernandez, E. M. *J. Biomed. Mater. Res. A* **2014**, *102*, 4244.
20. Khademhosseini, A.; Suh, K. Y.; Yang, J. M.; Eng, G.; Yeh, J.; Levenberg, S.; Langer, R. *Biomaterials* **2004**, *25*, 3583.
21. Hynes, S. R.; Rauch, M. F.; Bertram, J. P.; Lavik, E. B. *J. Biomed. Mater. Res. A* **2009**, *89*, 499.
22. Friedman, H. S.; Kerby, T.; Calvert, H. *Clin. Cancer. Res.* **2000**, *6*, 2585.
23. Ciucurel, E. C.; Sefton, M. V. *J. Biomater. Sci. Polym. Ed.* **2011**, *22*, 2515.
24. Hui-Bon-Hoa, G.; Kaddour, H.; Vergne, J.; Kruglik, S.; Maurel, M.-C. *BMC Biophys.* **2014**, *7*, 2.
25. Young, R. J.; Lovell, P. A. In Introduction to Polymers; 3rd ed.; CRC Press: Boca Raton, **2011**.
26. Canal, T.; Peppas, N. A. *J. Biomed. Mater Res.* **1989**, *10*, 1183.
27. Peppas, N. A.; Merrill, E. W. *J Appl. Polym. Sci.* **1977**, *21*, 1763.
28. Griffith, C. L.; Lopina, S. T. *Macromolecules* **1995**, *28*, 6787.
29. Kurdikar, D. L.; Peppas, N. A. *Macromolecules* **1994**, *27*, 733.
30. Mahoney, M. J.; Anseth, K. S. *Biomaterials* **2006**, *27*, 2265.
31. Kaufman, L. J.; Brangwynne, C. P.; Kasza, K. E.; Filippidi, E.; Gordon, V. D.; Deisboeck, T. S.; Weitz, D. A. *Biophys. J.* **2005**, *89*, 635.
32. Tibbitt, M. W.; Kloxin, A. M.; Sawicki, L. A.; Anseth, K. S. *Macromolecules* **2013**, *46*, 2785.
33. Zhu, J.; Beamish, J. A.; Tang, C.; Kottke-Marchant, K.; Marchant, R. E. *Macromolecules* **2006**, *39*, 1305.
34. Munoz-Pinto, D. J.; Samavedi, S.; Grigoryan, B.; Hahn, M. S. *Polymer* **2015**, *77*, 227.
35. Banerjee, A.; Arha, M.; Choudhary, S.; Ashton, R. S.; Bhatia, S. R.; Schaffer, D. V.; Kane, R. S. *Biomaterials* **2009**, *30*, 4695.
36. Welch, D. R.; Sakamaki, T.; Pioquinto, R.; Leonard, T. O.; Goldberg, S. F.; Hon, Q.; Erikson, R. L.; Rieber, M.; Rieber, M. S.; Hicks, D. J.; Bonventre, J. V.; Alessandrini, A. *Cancer Res.* **2000**, *60*, 1552.
37. Fischer, D.; Li, Y.; Ahlemeyer, B.; Krieglstein, J.; Kissel, T. *Biomaterials* **2003**, *24*, 1121.
38. Arnold, L. J.; Dagan, A.; Gutheil, J.; Kaplan, N. O. *Proc. Natl. Acad. Sci.* **1979**, *76*, 3246.
39. Edmondson, R.; Broglie, J. J.; Adcock, A. F.; Yang, L. *Assay Drug Dev. Technol.* **2014**, *12*, 207.
40. Ruoslahti, E.; Pierschbacher, M. D. *Science* **1987**, *238*, 491.
41. Rao, S. S.; Winter, J. O. *Front. Neuroeng.* **2009**, *2*, 1.
42. Zhu, J.; Tang, C.; Kottke-Marchant, K.; Marchant, R. E. *Bioconjug. Chem.* **2009**, *20*, 333.